Ontogeny of the Ptychaspidid Trilobite *Quadraticephalus elongatus* Kobayashi, 1935 from the Furongian (late Cambrian) Hwajeol Formation, Korea

ONTOGENY OF THE PTYCHASPIDID TRILOBITE *QUADRATICEPHALUS ELONGATUS* KOBAYASHI, 1935 FROM THE FURONGIAN (LATE CAMBRIAN) HWAJEOL FORMATION, KOREA

JI-HOON KIHM,[1,2] TAE-YOON PARK,[2] AND DUCK K. CHOI[1]

[1]School of Earth and Environmental Sciences, Seoul National University, Seoul 151–747, Korea, <jhkihm85@kopri.re.kr>; <dkchoi@snu.ac.kr>;
and [2]Division of Polar-Earth System Sciences, Korea Polar Research Institute, Incheon 406–840, Korea, <taeyoon.park@hotmail.com>

ABSTRACT—The development of the trilobite pygidium involves both an articulation process at the frontal part and the formation of new segments at the rear end, and hence the development of the meraspid pygidium entails complicated morphological changes. This study deals with the ontogeny of the Furongian (late Cambrian) ptychaspidid trilobite, *Quadraticephalus elongatus* (Kobayashi, 1935), from the Hwajeol Formation of the Taebaek Group, Taebaeksan Basin, Korea, with a special focus on the segmentation process during the meraspid pygidial development. Compared to the ontogeny of a ptychaspidid trilobite, *Asioptychaspis subglobosa* (Sun, 1924), which is assumed to be an ancestral species of *Q. elongatus*, the convexity of the cranidium of *Q. elongatus* increased in a slower rate; the yoked free cheek of *Q. elongatus* splits to form a ventral median suture in a later developmental stage; and, a rim-like ridge, which disappeared in the early holaspid pygidium of *A. subglobosa*, was maintained in the late holaspid period of *Q. elongatus*. These morphological changes with growth imply that paedomorphosis was involved in the evolution of *Q. elongatus*. Eleven stages are recognized for the meraspid pygidial development, which began with an accumulation phase during which the number of segments increased from three to seven, followed by an equilibrium phase with seven segments, and ended up with a depletion phase during which the number of segments within the pygidium decreased to four. During the depletion phase, the pygidial length did not increase or even slightly decreased. The onset of the epimorphic phase, in which the total number of trunk segments does not increase anymore, precedes the onset of the holaspid period, demonstrating that the developmental mode of *Q. elongatus* is protomeric.

INTRODUCTION

TRILOBITE ONTOGENY has been traditionally divided into the protaspid, meraspid, and holaspid periods, based on the development of articulated joints in the trunk region (Chatterton and Speyer, 1997). In the meraspid period, the anterior-most segment in the pygidium was released into the thoracic region at each molting, while new segments were formed at the rear end of the pygidium (Chatterton and Speyer, 1997). When trilobites attained the final number of thoracic segments, the segment release from the pygidium ceased, but the cessation of the new segment formation at the rear end did not always concurrently occur. Hughes et al. (2006) proposed a novel ontogenetic scheme which focuses on the generation of trunk segments: an anamorphic phase during which the number of segments increased and an epimorphic phase during which the number of segments did not increase anymore. Because the meraspid pygidium is where both segment release and segment formation took place during development, the growth pattern of meraspid pygidium is not simple. One of the important research subjects in the study of trilobite ontogeny is to observe the ontogenetic development of the meraspid pygidium in the light of the segmentation process. Simpson et al. (2005) reported a complex segmentation process of meraspid pygidium of the Ordovician pliomerid trilobite *Hintzeia plicamarginis* Simpson et al., 2005. Park and Choi (2010a, 2011a) recognized a depletion phase in the pygidial development of *Cyclolorenzella convexa* (Resser and Endo in Endo and Resser, 1937) and *Haniwa quadrata* Kobayashi, 1933, in which the total number of segments in the pygidium decreased mainly because the generation of new segments in the posterior part of the pygidium could not compensate the release from the anterior part of the pygidium.

The middle to late Furongian Hwajeol Formation of the Taebaek Group, Taebaeksan Basin, Korea contains three trilobite biozones: the *Asioptychaspis* Zone, the *Quadraticephalus* Zone, and the *Eosaukia* fauna in ascending order (Sohn and Choi, 2007). Recently, the ontogeny of well-preserved silicified trilobites from the *Asioptychaspis* Zone have been described in detail: they include *Tsinania canens* (Walcott, 1905), *Asioptychaspis subglobosa* (Sun, 1924), and *Haniwa quadrata* Kobayashi, 1933 (Park and Choi, 2009, 2010b, 2011a). However, silicified trilobites from the overlying *Quadraticephalus* Zone remain to be studied.

The family Ptychaspididae was considered to belong to the Order Asaphida Salter, 1864 (Fortey and Chatterton, 1988; Fortey, 1997). Recently, several studies disputed the monophyly of the Order Asaphida, defined by Fortey and Chatterton (1988) and Fortey (1990). (Whittington, 2003, 2007; Park and Choi, 2009; 2010b; 2011a; Adrain et al., 2009). While reporting the ontogeny of the ptychaspidid trilobite, *A. subglobosa* Sun, 1924, from the *Asioptychaspis* Zone of the Hwajeol Formation, Park and Choi (2010b) demonstrated that the ventral median suture has been attained by a mode different from that previously suggested for the Order Asaphida by Fortey and Chatterton (1988), and suggested that the Ptychaspididae should be excluded from the Order Asaphida. Lately, Adrain (2011) placed the Ptychaspididae under Order Uncertain.

This study deals with the ontogeny of a ptychaspidid trilobite, *Quadraticephalus elongatus* Kobayashi, 1935, from the *Quadraticephalus* Zone of the Hwajeol Formation, Korea. Given the stratigraphic occurrences, comparable mature morphology, and similar ontogenetic development, *Q. elongatus* is assumed to be a descendant species of *A. subglobosa*. Special attention is given
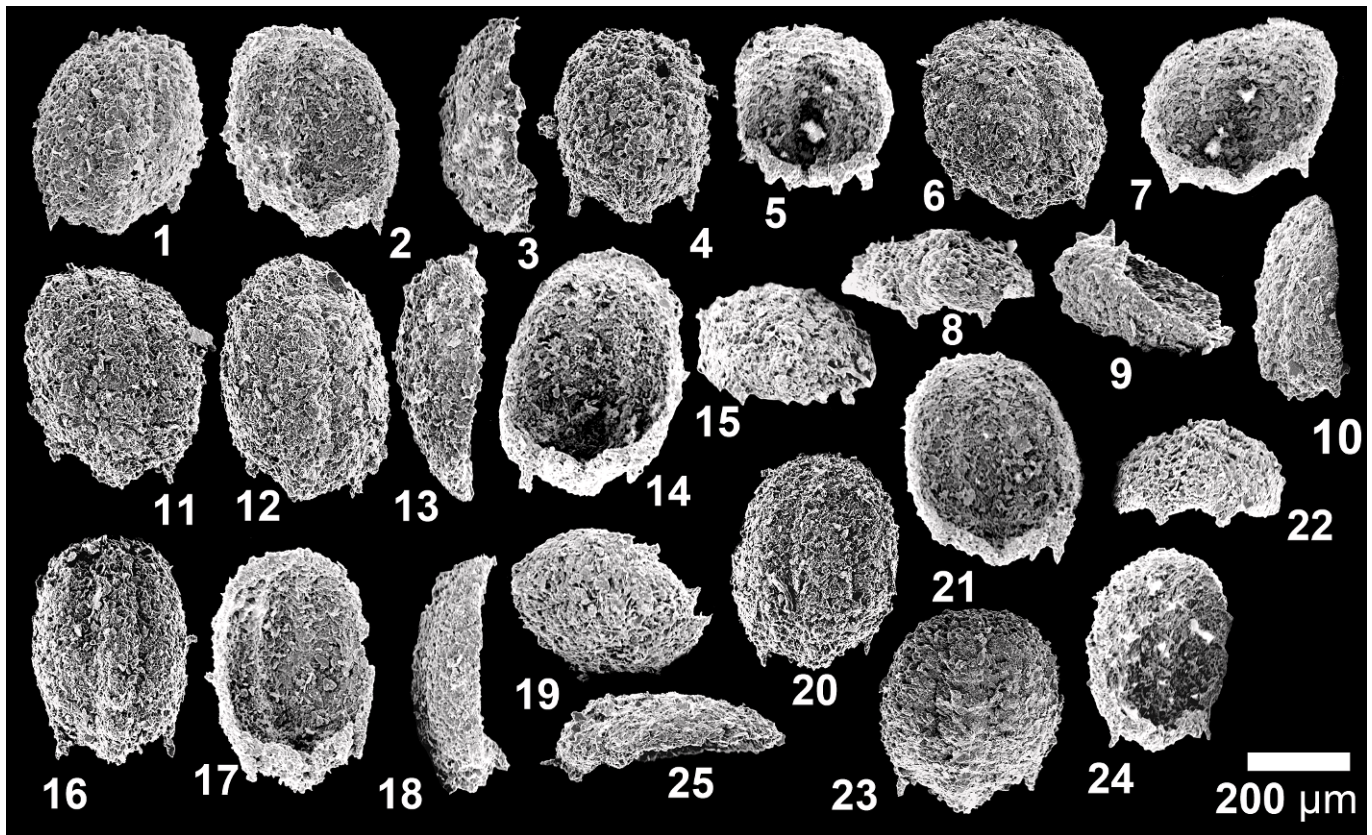
FIGURE *1*—Protaspides of *Quadraticephalus elongatus* (Kobayashi, 1935). *1–3*, SNUP6256, dorsal, ventral, and lateral views; *4, 5*, SNUP6257, dorsal and ventral views; *6–10*, SNUP6258, dorsal, ventral, posterior, oblique ventrolateral, and lateral views; *11*, SNUP6259, dorsal view; *12–15*, SNUP6260, dorsal, lateral, ventral, and posterior views; *16–19*, SNUP6261, dorsal, ventral, lateral, and oblique posterolateral views; *20–22*, SNUP6262, dorsal, ventral, and posterior views; *23–25*, SNUP6263, dorsal, ventral, and lateral views.

to the segmentation process during the pygidial development of *Q. elongatus*.

FOSSIL LOCALITY AND MATERIAL

All the material employed in this study was collected from the *Quadraticephalus* Zone of the lowermost part of the Hwajeol Formation at the Seokgaejae section, exposed along a forest road cut, approximately 12 km southeast of Taebaek City (for location see Lee and Choi, 2011, fig. 1). The Hwajeol Formation in this section measures ∼60 m in thickness with the lowermost part of the formation covered and hence the lowermost *Asioptychaspis* Zone of the formation is not recognized in the section (Choi et al. 2004; Sohn and Choi, 2007).

Limestone samples containing silicified trilobites were collected from the interval 3–8 m above the base of the exposed part of the formation. The rock samples were digested with 9% hydrochloric acid and silicified sclerites were secured from the residue. Collected trilobite sclerites belong to *Quadraticephalus elongatus* Kobayashi, 1935, *Lophosaukia orientalis* (Kobayashi, 1933), *Haniwa sosanensis* (Kobayashi, 1933), *Haniwa* sp., *Hamashania pulchera* (Kobayashi, 1942), *Akoldinioidia* sp., and *Micragnostus* sp. The sclerites of *Q. elongatus* employed in this study include 38 protaspides, 476 cranidia, 97 free cheeks, 259 pygidia, and 36 thoracic segments. All of the specimens illustrated in this study are deposited in the paleontological collections of Seoul National University with registered SNUP numbers.

ONTOGENY

Morphological terms employed in this study follow those of Whittington and Kelly (1997) and Chatterton and Speyer (1997), but the term 'meraspid pygidium' is used instead of transitory pygidium (see Hughes et al., 2006). The term 'equilibrium phase' and 'depletion phase' are also used instead of stasis phase and shedding state, respectively (see Simpson et al., 2005). Sagittal length and transverse width were measured for all protaspides, post-protaspid cranidia, and post-protaspid pygidia. A number of specimens suffered from tectonic distortion, to some extent, and thus any biologically meaningful clustering was not recognized from the length-width bivariate plots. However, meraspid pygidia were divided into 11 stages according to segment number and overall morphology.

Protaspid period.—The protaspides are ovoid in outline and measure 0.35–0.55 mm long and 0.34–0.48 mm wide (Fig. 1). The exoskeleton is convex with a steeply downsloping proto-pygidial region, and the axis becomes indistinct anteriorly. A pair of genal spines project rearward. The trunk is distinguished from the head by the posterior cranidial margin. In some, but not all, specimens, a pair of pygidial spines project ventrally (Fig. 1.8, 1.9).

Post-protaspid cranidial development.—Cranidia shorter than 0.50 mm (Fig. 2.1–2.4) are semi-oval in outline, with a parallel-sided glabella and deep axial furrows. The frontal area is not recognized in dorsal view, but is seen in oblique anterior view (Fig. 2.3), marked off by a faintly incised preglabellar furrow. The frontal part of the glabella downslopes steeply. Occipital ring

is convex, long medially, and clearly defined by a deep occipital furrow. Posterior cranidial border widens abaxially.

Cranidia of 0.50–0.64 mm in length (Fig. 2.5–2.7) are subtrapezoidal in outline. The frontal area is recognized in the dorsal view. Glabella tapers slightly forwards, and axial furrows are deeply incised. A short and tumid occipital spine projects posteriorly. The ventral margin is nearly straight in lateral view (Fig. 2.7).

Cranidia longer than 0.64 mm (Fig. 2.8–2.11) display a weakly recognizable frontal area in dorsal view. The convexity of the cranidia becomes stronger due to steeply downsloping frontal lobe (Fig. 2.10). Frontal area downslopes gently forwards. The lateral cranidial margin is sinuous, probably due to the appearance of the palpebral lobes.

In cranidia of 0.79–1.2 mm in length (Fig. 2.12–2.16), the cranidial outline becomes almost trapezoidal, with a more-or-less straight anterior cranidial margin. Frontal area is well-recognized in dorsal view (Fig. 2.12) and steeply downsloping anteriorly (Fig. 2.15). Palpebral lobes are 0.26–0.29 of the cranidial length. Fingerprint-like prosopon is weakly developed on the glabellar surface (Fig. 2.12). S1 and S2 glabellar furrows are faintly indicated. Posterior border furrow is nearly straight and posterior cranidial border does not widen as much abaxially as that of smaller cranidia.

In cranidia longer than 1.22 mm (Fig. 2.17–2.21), the anterior margin of the frontal area is more broadly rounded. Palpebral lobes are relatively longer, 0.33–0.36 of the cranidial length. Palpebral furrows are clearly impressed. Fingerprint-like prosopon is distinct on the glabella front though is not expressed on the internal surface, but is weakly impressed on the posterior part of the genal field and occipital ring (Fig. 2.17, 2.18). S1 and S2 furrows are clearly incised.

In the cranidia of 1.54–2.60 mm long (Fig. 2.22–2.26), the fingerprint-like prosopon is clearly developed on the whole surface of the glabella, genal field, and occipital ring. Linear ornamentations are faintly developed on the surface of the palpebral lobe and the frontal area. The S1 and S2 glabellar furrows are moderately impressed. Palpebral lobes are 0.37–0.39 of the cranidial length. The abaxially widening posterior border is slightly bent posteriorly. The occipital ring is rectangular in outline, with the occipital spine obliquely directed posteriorly. The relative size of the occipital spine at this stage is the largest among the whole developmental stages.

Cranidia of 2.60–3.3 mm long (Fig. 3.1–3.4) have laterally convex anterior branches of the facial suture. Palpebral lobes and occipital spine become relatively short; palpebral lobes are 0.31–0.34 of the total length of the cranidia. Occipital spine projects upward. While the convexity of the whole cranidia does not change much, the frontal area continues to become longer. The surface ornamentation including the fingerprint-like prosopon is less distinct and not recognized on the surface of the palpebral lobes. S1 and S2 glabellar furrows are faintly indicated. An extremely faint impression is recognizable in the place where the S3 glabellar furrow would be expected (Fig. 3.1). The posterior cranidial margin runs abaxially straight from the flank of the occipital ring, and then is abruptly directed obliquely rearward.

In the cranidia longer than 3.3 mm (Fig. 3.5–3.8), the frontal area is relatively long. The overall convexity is slightly less than that of the smaller cranidia (Fig. 3.5). The ornamentation on the surface including the fingerprint-like prosopon becomes less distinct; it is reduced in relief and recognized only on the surface of the frontal lobe of glabella, frontal area, and the posterior part of the genal field. Palpebral lobes become relatively shorter; less than 0.3 of the cranidial length. Glabellar furrows are more clearly incised. The occipital spine is subdued.

Free cheek development.—Free cheeks are yoked during the earlier phases of development (Fig. 4.1–4.6). The smallest free cheek available (Fig. 4.1–4.3) has a simple morphology with moderately long and broad librigenal spines. The genal spines are relatively short, 0.32–0.35 of the whole free cheek length. The librigenal field is narrow.

With growth, the librigenal fields become broader and the genal spines become relatively longer, 0.40–0.44 of the whole free cheek length (Fig. 4.5, 4.6). The genal spines are weakly curved abaxially toward the posterior tip. Ridge-like prosopon running subparellel to the outer margin is faintly recognized on the surface of the librigenal field.

Free cheeks longer than 2.5 mm (Fig. 4.7, 4.8) represent the splitting of the previously yoked free cheek. This mode of ventral median suture formation is the same as that of the ptychaspidid trilobite, *A. subglobosa* (Park and Choi, 2010a). The anterior part of doublure is inturned, forming a tube-like appearance. The outward curvature of the genal spine is prominent (Fig. 4.7)

As the free cheeks grow (Fig. 4.9–4.21), the librigenal field becomes broad. The ridge-like prosopon is well-developed on the abaxial part of the librigenal field and extends onto the whole part of the genal spine. Of the ridges, two or three ridges are prominent along the paradoublural line.

Thoracic segment development.—Two thoracic segment-articulated morphologically immature specimens (Fig. 5) help us to understand the anterior-posterior aspect of the thoracic segments within an individual as well as the immature thoracic segment morphology. The anteriormost thoracic segment has a broader articulating facet than those posterior to it (Fig. 5.1, 5.2).

Small thoracic segments are generally transverse in dorsal view (Fig. 6.1–6.10) each with a convex axial ring. The axis is 0.35–0.40 of the entire width of the thoracic segment. The axial spine is broad-based, long, and weakly curved forward or upward. The lateral tip of some of the thoracic pleurae has an obliquely truncated end (Fig. 6.8). In large specimens (Fig. 6.11–6.19), the axial spine is longer, 0.28–0.33 of the height of the thoracic segment (Fig. 6.13), which is directed upward and rearward, showing the opposite orientation to that of smaller thoracic segments (compare Fig. 6.3, 6.8 with 6.13, 6.17). Panderian processes are recognized in anterior view (Fig. 6.11, 6.14). The lateral tip of the pleurae is weakly pointed (Fig. 6.13, 6.17). Given the morphology of a complete specimen of degree 6 meraspis (Fig. 5.1–5.4), there is a tendency that the axial spine reaches its maximum length in the fifth thoracic segment, and is progressively shorter in the anterior and posterior to the fifth segment. Thus the posterior-most thoracic segment in the morphologically immature holaspid specimen (Fig. 5.5, 5.6) has no trace of axial spine at all.

Post-protaspid pygidial development.—The mature pygidia of *Quadraticephalus elongatus* observed in this study have a different morphology from those described by Sohn and Choi (2007, figs. 5, N, P, T and U). The pygidia illustrated by Sohn and Choi (2007) belong to *Haniwa* as pointed out by Park and Choi (2011a). Based on the morphology including the number of axial rings within a meraspid pygidium, the meraspid pygidia are divided into 11 stages. This is also concordant to a morphologically mature complete holaspid specimen with 11 thoracic segments of *Quadraticephalus* (see Zhang and Jell, 1987, pl. 114, fig. 1). Counting the number of pygidial segments may be difficult due to the ambiguity caused by the rear end of axis where new segments are proliferated. In this study, only obviously recognizable segments were counted, and the ambiguous last segment is referred as the terminal piece.

Pygidia of stage A (Fig. 7.1–7.3; N=3) are inverted subtrapezoidal in outline with medially indented posterior margin and are approximately twice wide as long. The smallest trunk is
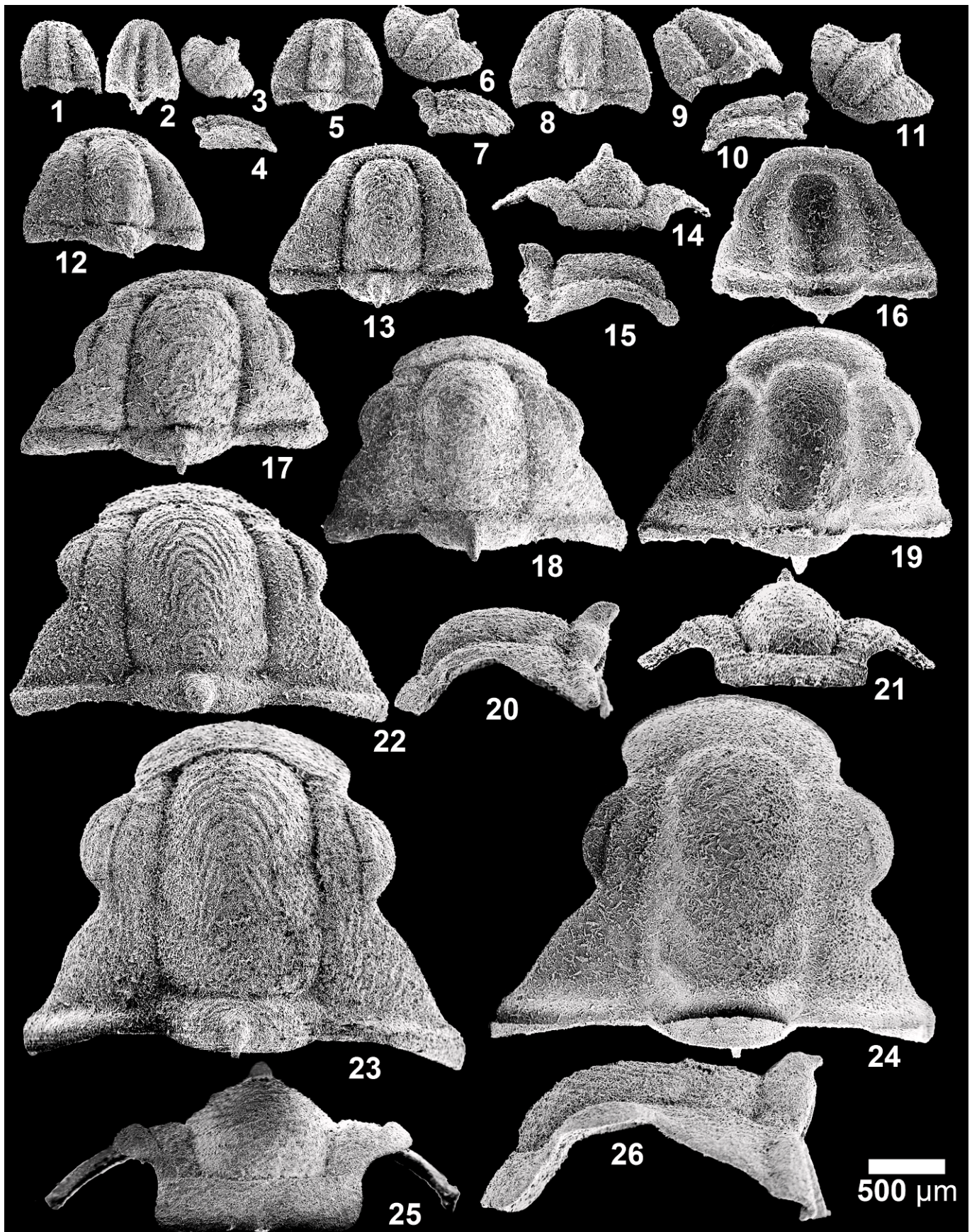
FIGURE *2*—Post-protaspid cranidia of *Quadraticephalus elongatus* (Kobayashi, 1935). *1–4*, SNUP6264, dorsal, ventral, oblique anterolateral, and lateral views; *5–7*, SNUP6265, dorsal, oblique anterolateral and lateral views; *8–11*, SNUP6266, dorsal, oblique posterolateral, lateral, and oblique anterolateral views; *12*,
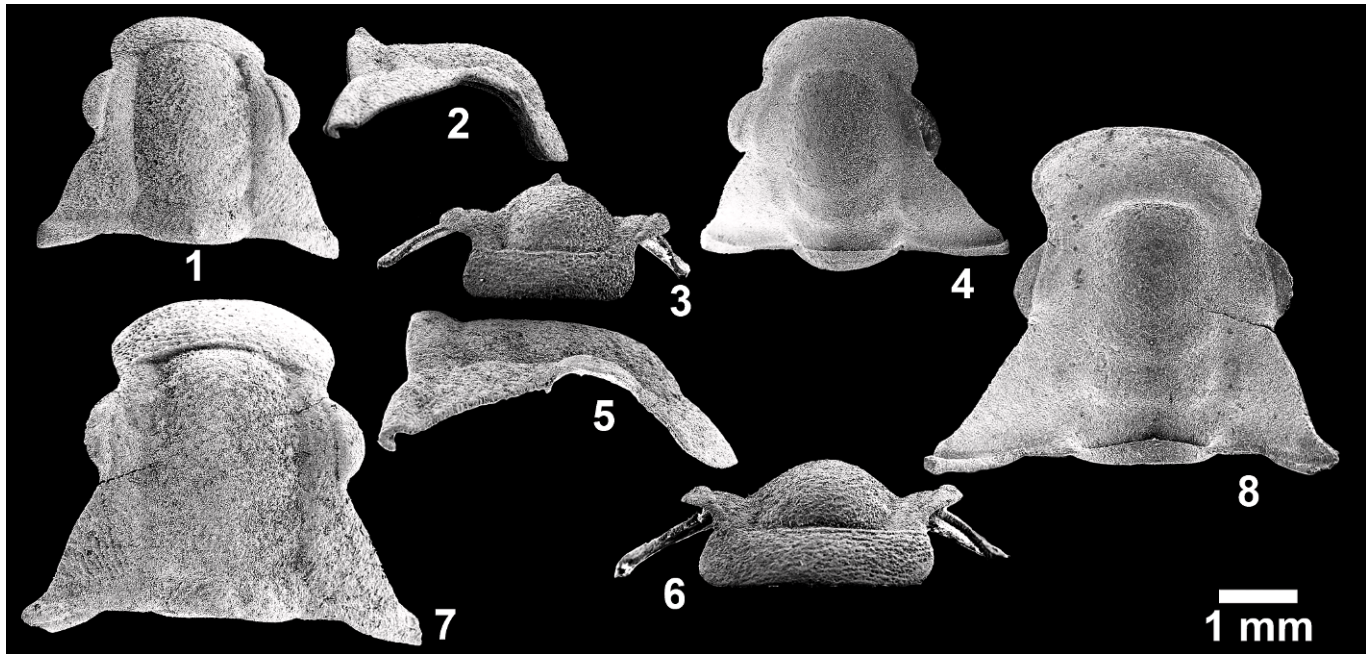
FIGURE *3*—Post-protaspid cranidia of *Quadraticephalus elongatus* (Kobayashi, 1935). *1–4*, SNUP6273, dorsal, lateral, anterior, and ventral views; *5–8*, SNUP6274, dorsal, lateral, anterior, and ventral views.

0.22 mm long and 0.40 mm wide. Although the specimens are not so well-preserved to reveal morphologic details, it appears to have three axial rings with a short axial spine that projects anteriorly. A pair of spines at the posterior margin of trunk is weakly curved adaxially.

Pygidia of stage B (Fig. 7.4–7.6; N=14) possess four axial rings and are subrectangular in outline and longer than wide (Fig. 7.4). The lateral margins are convex. The articulating half ring is clearly visible. The pleural and interpleural furrows are weakly incised. A pair of posterior marginal spines is present. In lateral view (Fig. 7.6), the axial spines are prominent.

Pygidia of stage C (Fig. 7.7–7.9; N=30) have five axial rings. They are similar to those of stage B, but develop a narrow marginal border (Fig. 7.8). The border is of low convexity, clearly recognizable in dorsal view (Fig. 7.7). The pair of posterior marginal spines has now disappeared. The axial spines become longer. In ventral view, the doublure become wider along the posterior margin than that at the lateral margin (Fig. 7.9).

Pygidia of stage D (Fig. 7.10, 7.11; N=48) are semi-circular in outline. The pleural and interpleural furrows are distinctly impressed. The pygidial border is developed. With the increase of the convexity, the anteromost axial spine is now directed upwards and forwards. The posterior margin displays a weak median indentation.

In the stage E (Fig. 7.12–17.16; N=47), the pygidia bear six axial rings and are wider than long. The pleural and the interpleural furrows are more clearly impressed. The pygidial border has become wider and steeper, with a rim along the edge of the pleural field (Fig. 7.12). In lateral view, the posterior part of the pygidial border is slightly thicker than it is in the anterior part (Fig. 7.13, 7.16). The anteriormost axial spine is the longest; in the earlier stages, the spine is shorter than or is similar in length to other spines (Fig. 7.13). Some specimens display a serrated

ventral margin (Fig. 7.16), which corresponds to spinose lateral end of thoracic pleurae.

Pygidia of stage F (Fig. 7.17–7.20; N=23) have seven axial rings and a terminal piece and are semi-circular in outline. The axial spines have become shorter and the posteriormost axial spine is hard to recognize. On the lateral view, the serrated ventral margin displays six marginal spines, indicating that the trunk at this stage has six protothoracic segments (Fig. 7.19, 7.20). The equilibrium phase begins with this stage.

In stage G (Fig. 7.21, 7.22; N=11), the pygidial border becomes prominent and the rim is strongly raised; the serrated ventral margin is also visible in dorsal view; and anterior spines are longer and more distinct. The anteriormost spine is curved posteriorly, unlike that in stage F. Five protothoracic segments are recognized. The pygidial morphology is nearly identical to that of meraspid degree 6 specimens (Fig. 5.1–5.4), indicating that the stage G corresponds to the meraspid degree 6.

The stage H (Fig. 7.23–7.25; N=8) is the last stage of the equilibrium phase. The pygidial morphology of this stage is similar to that of stage G except for possession of four protothoracic segments.

From stage I (N=11), the number of the axial rings is reduced and thus this stage corresponds to the onset of the depletion phase (sensu Simpson et al. 2005). The pygidia of stage I (Fig. 7.26–7.28) have six axial rings and a terminal piece. The axial spines become notably shorter and so only the anteromost one is visible. The high pygidial border becomes inclined adaxially and forwardly, so that the highest contour of the border shows a rim-like ridge. Pygidia of stage I have three protothoracic segments (Fig. 7.27).

In sequential growth, the pygidia of stage J (Fig. 7.29–7.31; N=7) release one protothoracic segment while retaining six axial
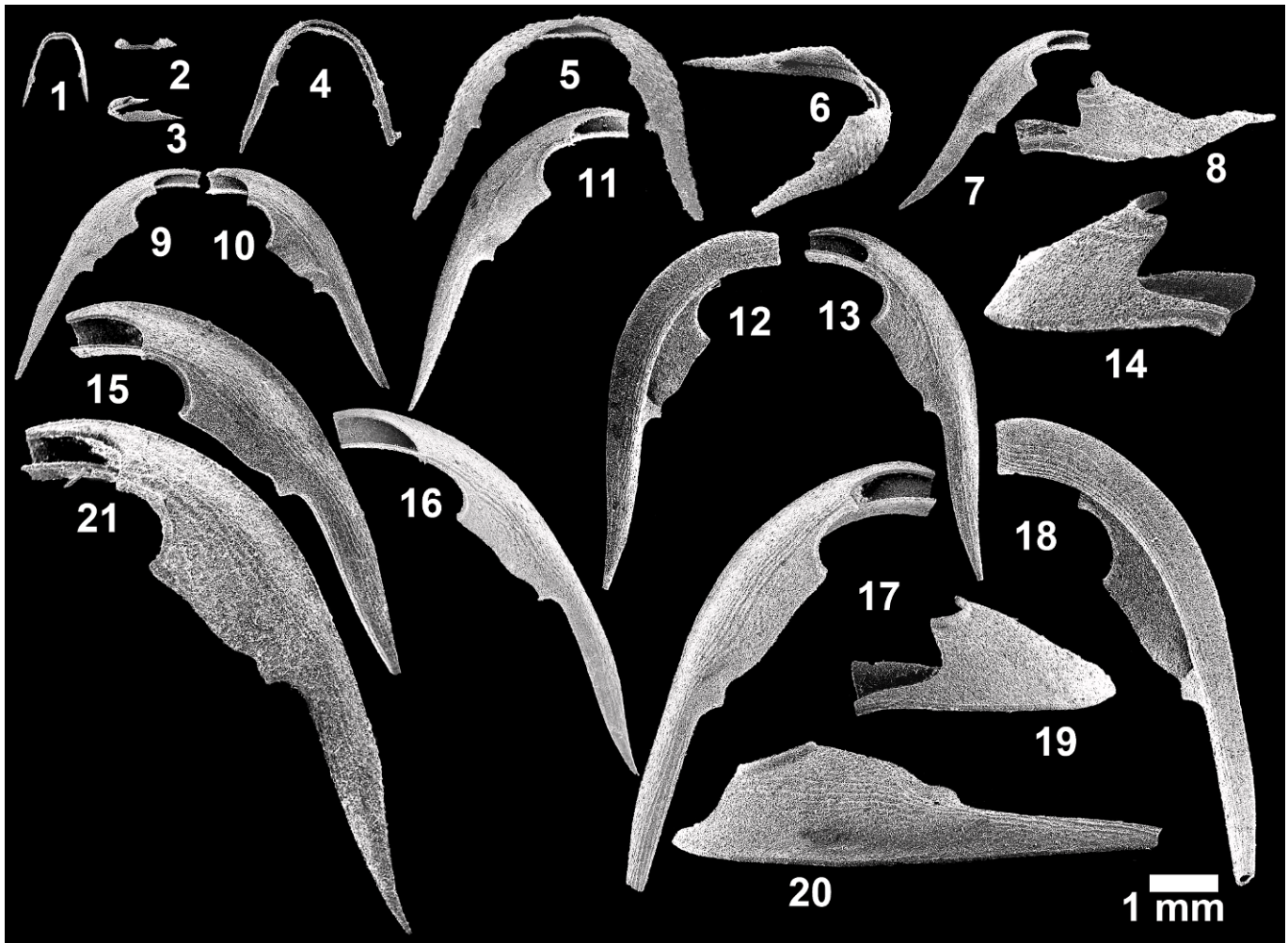
←

SNUP6267, dorsal view; *13–16*, SNUP6268, dorsal, anterior, lateral, and ventral views; *17*, SNUP6269, dorsal view; *18–21*, SNUP6270, dorsal, ventral, lateral, and anterior views; *22*, SNUP6271, dorsal view; *23–26*, SNUP6272, dorsal, ventral, anterior, and lateral views.

FIGURE 4—Free cheeks of *Quadraticephalus elongatus* (Kobayashi, 1935). *1–6*, yoked-form free cheeks of early developmental phase: *1–3*, SNUP6275, dorsal, anterior, and oblique lateral views; *4*, SNUP6276, dorsal view; *5, 6*, SNUP6277, dorsal and oblique lateral views; *7–21*, split-form free cheeks of late developmental phase: *7, 8*, SNUP6278, dorsal and lateral views; *9*, SNUP6279, dorsal view; *10*, SNUP6280, dorsal view; *11*, SNUP6281, dorsal view; *12–14*, SNUP6282, ventral, dorsal, and anterior views; *15*, SNUP6283, dorsal view; *16*, SNUP6284, dorsal view; *17–20*, SNUP6285, dorsal, ventral, anterior, and lateral views; *21*, SNUP6286, dorsal view.

rings and a terminal piece, leaving only two protothoracic segments.

Pygidia of stage K (Fig. 7.32–7.34; N=12) have five axial rings and a terminal piece. The rim along the pleural field is strongly raised. The axial spines can no longer be recognized (Fig. 7.33). Only one protothoracic segment is present.

Pygidia with four axial rings and a terminal piece (Fig. 7.35–7.38) show no trace of protothoracic segments in lateral view (Fig. 7.37), hence they are entering into the holaspid period. The inter-ring furrows, pleural furrows and interpleural furrows become weakly impressed and eventually disappear (Fig. 8). The rim-like ridge along the pleural field becomes weaker and terrace lines parallel to the pygidial margin appear in the border and doublure (Fig. 8.6, 8.8). The anterior margin is nearly transverse (Fig. 8.6), hence corresponding to extremely low curvature in the posteriormost thoracic segment, as mentioned above.

ONTOGENETIC COMPARISON WITH *ASIOPTYCHASPIS SUBGLOBOSA*

The ontogeny of *Asioptychaspis subglobosa* (Sun, 1924), a probable ancestral species of *Q. elongatus*, has already been described (Park and Choi, 2010b), and thus a detailed comparison of the ontogeny of the two species is available. It

is also possible to examine whether some of the morphologically novel features of *Q. elongatus* were induced by heterochronic changes during development. This study assumes that specimens of the two species with similar size represent a comparable developmental stage.

Protaspides.—The protaspides of *Asioptychaspis subglobosa* were divided into two stages; the early and the late stages (Park and Choi, 2010b). In contrast, the protaspides of *Quadraticephalus elongatus* cannot be divided into distinct stages. Interestingly, the size and overall morphology of the protaspides of *Q. elongatus* are closely similar to those of the early stage protaspides of *A. subglobosa*. Although the presence of both genal and pygidial spines in some of the protaspides of *Q. elongatus* is rather comparable to that of the late stage protaspides of *A. subglobosa*, the overall shape and morphology such as relatively indistinct axial furrows are comparable to those of the early stage protaspides of *A. subglobosa* (see Park and Choi, 2010b, fig. 3). Moreover, some early stage protaspides of *A. subglobosa* also display both genal and pygidial spines (Park and Choi, 2010b, fig. 3.7–3.9). With subsequent molting, an articulation appeared in *Q. elongatus*, indicating that this species has entered into the meraspid period, while the morphologically comparable early stage protaspides of *A. subglobosa* developed
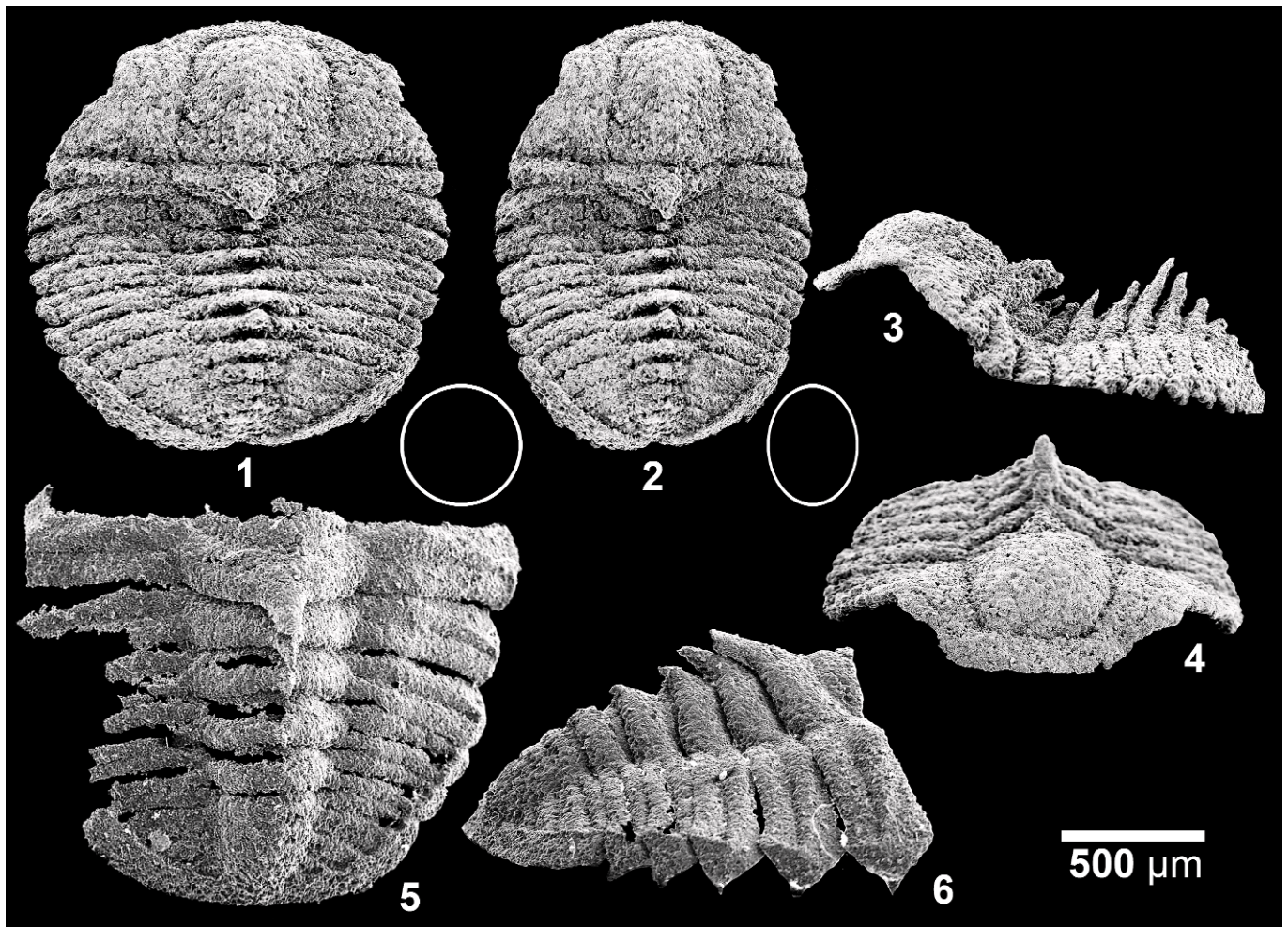
FIGURE 5—Meraspid degree 6 exoskeleton of *Quadraticephalus elongatus* (Kobayashi, 1935) retaining the trunk, with free cheeks missing. *1, 3, 4*, original meraspid specimen that is considered to have been deformed only laterally in a single planar direction: *1*, SNUP6287, dorsal view; *2*, with Adobe Photoshop, the specimen image in *Figure 6.1* is compressed along the sagittal axis, the laterally compressed white circle represents the amount of compression; *3*, lateral view; *4*, anterior view; *5, 6*, fragmentary holaspid specimen of *Q. elongatus* which consists of the pygidium and the five posterior-most thoracic segments, SNUP6288, dorsal and lateral views.

into the late stage protaspides with the articulation not yet appeared. This is well represented in the bivariate plots of the protaspides of both species and the earliest meraspid cranidia of *Q. elongatus* (Fig. 9). This means that the first articulation appeared earlier in *Q. elongatus* than in *A. subglobosa*.

The discrepancy in the timing of the first articulation in these two closely related trilobite species is significant in respect of the issue raised by Park and Choi (2011b). Because the protaspid morphology of related taxa tends to be more similar to each other than to those of less closely related taxa, the protaspid morphology has long been employed to determine the phylogenetic relationship and higher-level classification without any logical justification. Park and Choi (2011b), however, pointed out that there is a logical pitfall in just comparing the protaspid morphology of different taxa, because the timing of the first articulation which differentiates the meraspid period from the protaspid period is not necessarily the same among different trilobite taxa: closely related species may display a different timing of the first articulation. The fact that the single-staged protaspides of *Q. elongatus* correspond to the early stage protaspides of *A. subglobosa* corroborates Park and Choi (2011b)'s argument. Although *A. subglobosa* and *Q. elongatus* have a close phylogenetic relationship, there is a clear

discrepancy in the timing of the first articulation between the two species. The late stage protaspides of *A. subglobosa* are more homologous to the first meraspid stage, not the protaspid stage, of *Q. elongatus*. Therefore, as noted by Park and Choi (2011b), care must be taken when using protaspid morphology for phylogenetic relationship of trilobites.

Post-protaspid cranidia.—One of the most notable differences between the cranidia of *Q. elongatus* and *A. subglobosa* is the convexity of the cranidium. The earliest cranidial morphology is similar in these two species. With growth, however, the convexity of the cranidia of the two species becomes gradually disparate from each other: the convexity of *A. subglobosa* changes more radically during development than that *of Q. elongatus*, resulting in strongly bulbous frontal lobe of *A. subglobosa*. When comparing the ratio of the length of palpebral lobe to the cranidial length, the palpebral lobes attain a similar ratio in earlier developmental stages of *A. subglobosa*. However, with growth, palpebral lobes become comparatively smaller in *Q. elongates* than *A. subglobosa*.

Free cheeks.—Free cheeks of the two species display a similar developmental pattern. Park and Choi (2010b) presented three different modes of the ventral median suture (VMS) formation: *A. subglobosa* shows the third mode of VMS formation in which an initially yoked free cheek splits along the sagittal line during
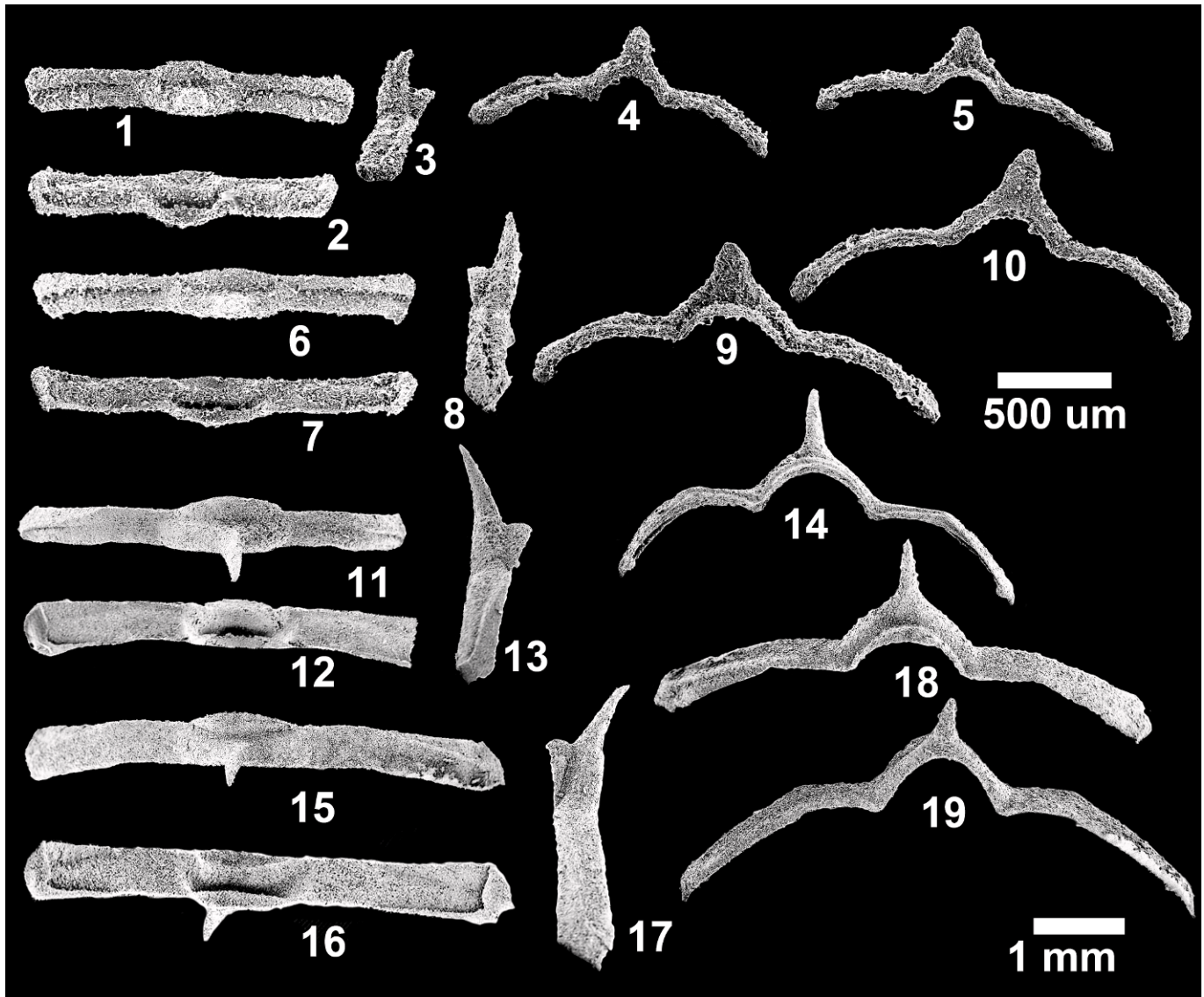
FIGURE *6*—Thoracic segments of *Quadraticephalus elongatus* (Kobayashi, 1935). *1–10*, thoracic segments at early developmental phase with 500 μm scale: *1–5*, SNUP6289, dorsal, ventral, lateral (anterior to the right), posterior, and anterior views; *6–10*, SNUP6290, dorsal, ventral, lateral (anterior to the left), anterior, and posterior views; *11–19*, thoracic segments at late developmental phase with 1mm scale: *11–14*, SNUP6291, dorsal, ventral, lateral (anterior to the right), and anterior views; *15–19*, SNUP6292, dorsal, ventral, lateral (anterior to the left), anterior, and posterior views.

development to form a VMS. *Quadraticephalus elongatus* also displays the same mode of VMS formation with *A. subglobosa*, but differs in the timing of the splitting. The largest yoked free cheek of *A. subglobosa* is 1.2 mm long, whereas that of *Q. elongatus* is 2.5 mm long, suggesting that the former attains the VMS in an earlier developmental stage (Fig. 10).

Post-protaspid pygidia.—Meraspid pygidia of both species show a similar segmentation pattern and morphology. The smallest specimens available for both species have three or four axial rings. In the subsequent development, the number of segments increases (accumulation phase) until there are seven segments within the pygidium (equilibrium phase). Subsequently, the number of segments within the pygidium decreases (depletion phase) until only four segments remain at the entry to the holaspid period. The meraspid pygidial morphology of the two species is also almost identical, but in the holaspid period the rim-like ridge of *Q. elongatus* is prominent throughout the holaspid period, whereas that of *A. subglobosa* remained in the earliest holaspid period only and subsequently disappeared.

In summary, the cranidial convexity change and the timing of free cheek-splitting during development indicate that the rate of morphological change is apparently slower in *Q. elongatus* than its ancestral species, *A. subglobosa*. Moreover, the mature pygidia of *Q. elongatus* retain the rim-like ridge which disappeared during the development in *A. subglobosa*. It can, therefore, be postulated that paedomorphosis must have been involved in the evolution of *Q. elongatus*.

SEGMENTATION PROCESS

The meraspid pygidia of *Quadraticephalus elongatus* undergo dynamic changes in the number of segments during development. Because the complete holaspid specimen of *Q. elongatus* has not been recovered, the final number of thoracic segments is unknown. However, a nearly complete specimen of *Quadraticephalus*, illustrated by Zhang and Jell (1987, pl. 114, fig. 1; described under the name of *Changia walcotti* Sun, 1924), has 11 thoracic segments. Given that the meraspid degree 6 specimens of *Q. elongatus* with a complete trunk (Fig. 5.1–
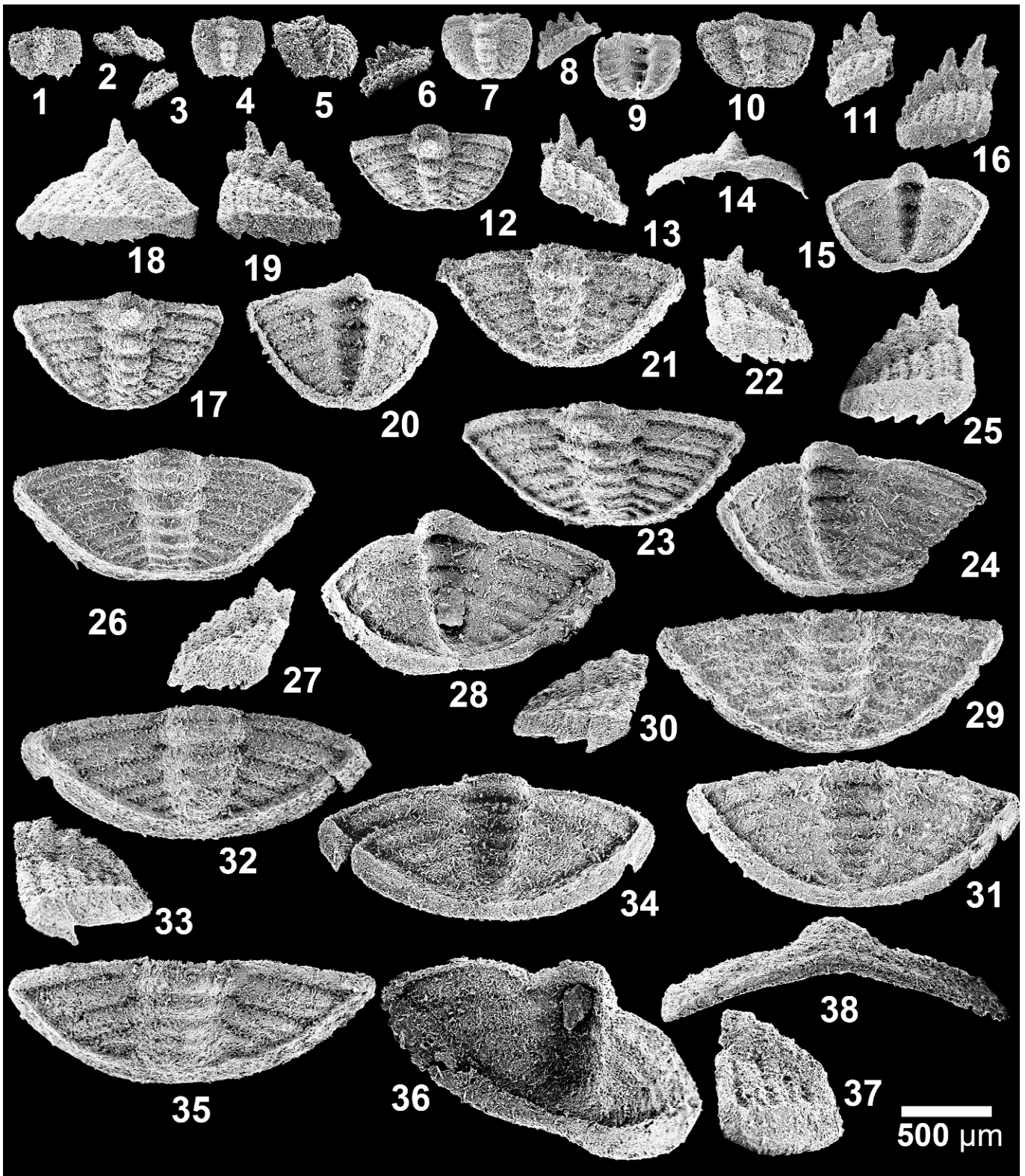
FIGURE 7—Post-protaspid pygidia of *Quadraticephalus elongatus* (Kobayashi, 1935). *1–20*, meraspid pygidia in accumulation phase: *1–3*, SNUP6293, Stage A, dorsal, oblique posterior, and lateral views; *4–6*, SNUP6294, Stage B, dorsal, oblique posterolateral, and lateral views; *7–9*, SNUP6295, Stage C, dorsal, lateral, and ventral views; *10, 11*, SNUP6296, Stage D, dorsal and lateral views; *12–15*, SNUP6297, Stage E, dorsal, lateral, posterior, and ventral views; *16*, SNUP6298, Stage E, lateral view; *17–20*, SNUP6299, Stage F, dorsal, posterolateral, lateral, and ventral views; *21–25*, meraspid pygidia in equilibrium phase: *21, 22*, Stage G, SNUP6300, dorsal and lateral views; *23–25*, SNUP6301, Stage H, dorsal, ventral, and lateral views; *26–34*, meraspid pygidia in depletion phase: *26–28*, SNUP6302, Stage I, dorsal, lateral, and ventral views; *29–31*, SNUP6303, Stage J, dorsal, lateral, and ventral views; *32–34*, SNUP6304, Stage K, dorsal, lateral, and ventral views; *35–38*, holaspid pygidium, SNUP6305, dorsal, ventrolateral, lateral, and posterior views.
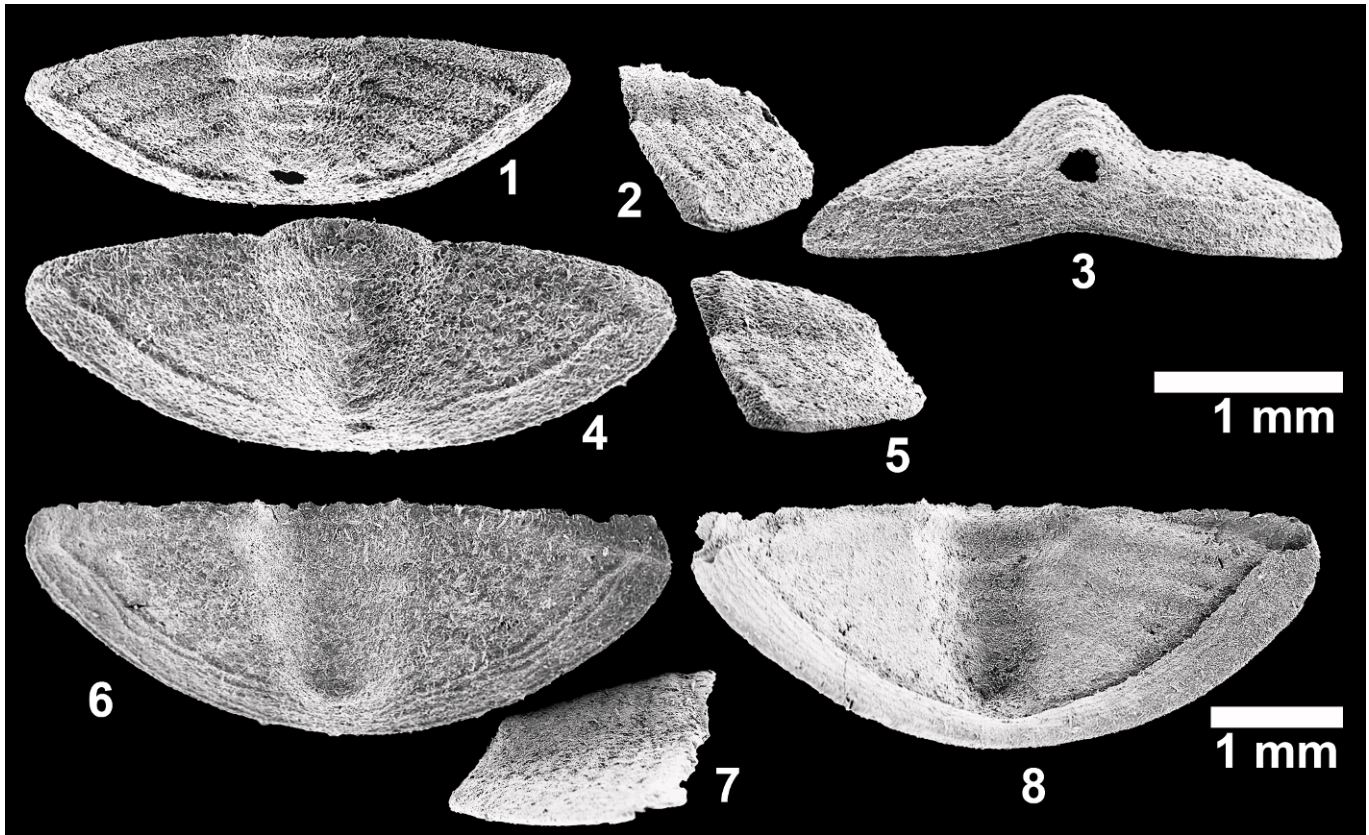
FIGURE 8—Holaspid pygidia of *Quadraticephalus elongatus* (Kobayashi, 1935). *1–3*, SNUP6306, dorsal, lateral, and posterior views; *4, 5*, SNUP6307, dorsal and lateral views; *6–8*, SNUP6308, dorsal, lateral, and ventral views.

5.4) has a pygidial morphology similar to the pygidial developmental stage G, and four more pygidial developmental stages are differentiated after the stage G before entering into the holaspid period, *Q. elongatus* must have had 11 thoracic segments in the holaspid period (Fig. 11).

The meraspid pygidia of *Q. elongatus* increase in length and width during the period from the stage A to F, and this period corresponds to an accumulation phase during which the number of segments within the pygidium increases from three to seven (Fig. 11). During the stage F–H, the meraspid pygidial development enters into an equilibrium phase during which the number of segments within the pygidium does not change (Fig. 11). The rate of sagittal length increase of the pygidium slows down during these stages (Fig. 12). Subsequently, the formation of new segments at the rear end of the pygidium ceased, but the release of thoracic segments at the anterior of the pygidium was maintained. Accordingly, the number of segments decreases down to four in the pygidium, representing a depletion phase (Fig. 11). During this phase, the sagittal length of the pygidium does not increase nor slightly decreases, while the transverse width increases (Fig. 12). It can be inferred that increase of the length due to the size increase of pygidial segments could not compensate the decrease of length caused by release of the anteriormost segment into the thorax. Such stagnancy in size during pygidial development has been reported in several trilobite species including *Hintzeia plicamarginis* Simpson et al., 2005 (Simpson et al., 2005), *Cyclolorenzella convexa* (Resser and Endo in Endo and Resser, 1937) (Park and Choi, 2010a), and *Haniwa quadrata* Kobayashi, 1933 (Park and Choi, 2011a). All of these cases have been considered to be related to the presence of a depletion phase during pygidial
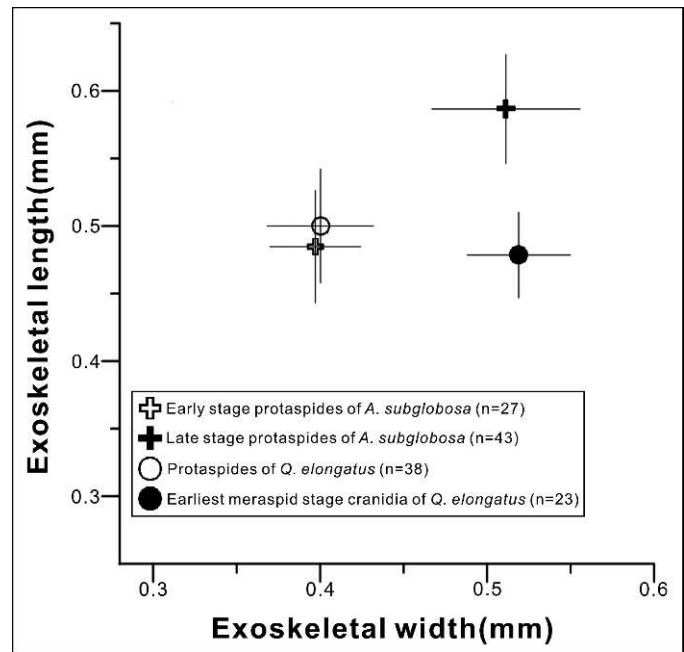

FIGURE 9—The mean scores of the protaspid size of *Quadraticephalus elongatus* (Kobayashi, 1935) and *Asioptychaspis subglobosa* (Sun, 1924), and the earliest meraspid stage size of *Q. elongatus*. One standard deviation bars are extended to horizontal and vertical side of the mean. It is noticeable that the size of the early stage protaspides of *A. subglobosa* is similar to that of the singe staged-protaspides of *Q. elongatus*, and the earliest meraspid stage cranidia of *Q. elongatus* show similar width to the late stage protaspides of *A. subglobosa*. This implies that the first articulation appeared earlier in development for *Q. elongatus*.
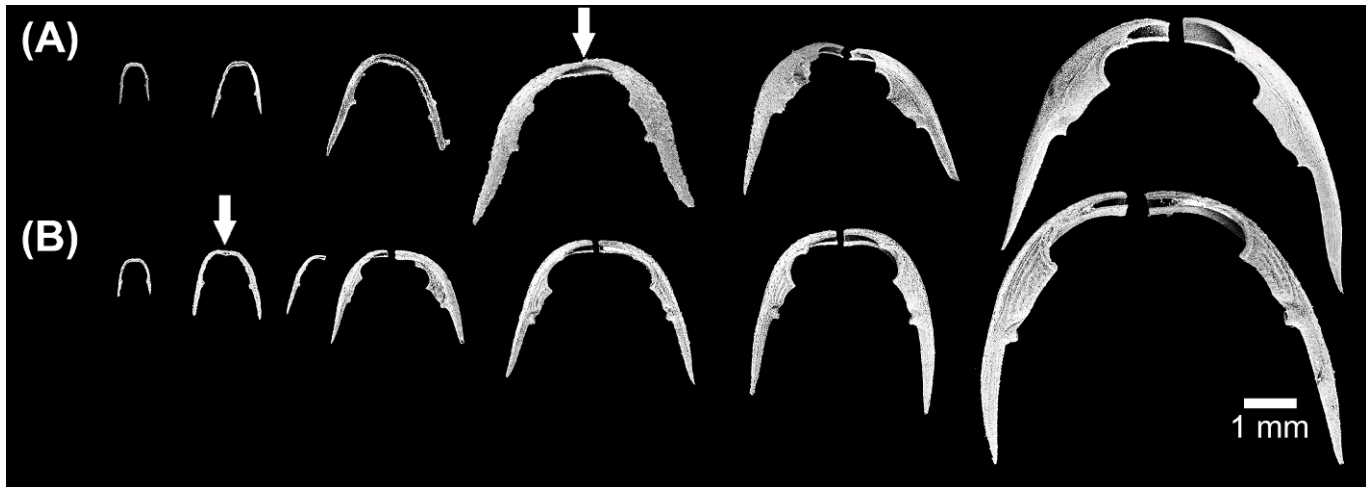
FIGURE 10—Comparison of the development of free cheek between *Quadraticephalus elongatus* (Kobayashi, 1935) (*A*) and *Asioptychaspis subglobosa* (Sun, 1924) (*B*). The splitting timing of the initially yoked free cheek of *Q. elongatus* is later in development, compared that of *A. subglobosa*. The white arrows represent the latest developmental stage of each species, in which the free cheeks remained yoked.

development. It is noteworthy that the depletion phase has been recorded among phylogenetically remotely related trilobite lineages. In *Q. elongatus,* the total number of segments does not increase anymore since the stage J, and the holaspid period begins after stage K. Hence, the developmental mode of *Q. elongatus* is protomeric (sensu Hughes et al., 2006) in which the epimorphic phase precedes the onset of the holaspid period.

CONCLUSIONS

The ontogenetic study of *Quadraticephalus elongatus* makes it possible to compare its ontogenetic development with the probable ancestral species, *Asioptychaspis subglobosa* (Sun, 1924). The single-staged protaspides of *Q. elongatus* are considered homologous to the early stage protaspides of *A. subglobosa*. Subsequently, *Q. elongatus* entered into the earliest meraspid stage with the appearance of the first articulation, while the early stage protaspides of *A. subglobosa* developed into the late stage protaspides. This indicates that phylogenetically closely related trilobites could have a different timing of the first articulation, corroborating Park and Choi's (2011b) argument that protaspides of different trilobite species cannot always be regarded to be in a homologous stage. Although the earliest cranidial morphology of *A. subglobosa* is similar to that of *Q. elongatus*, the overall convexity increases more slowly in *Q. elongatus*. The free cheeks of *Q. elongatus* were initially

yoked, but subsequently split to form a ventral median suture as in *A. subglobosa*. However, the splitting occurred later in development in *Q. elongatus* than in *A. subglobosa*. The two species display a similar meraspid pygidial development, but the rim-like ridge did not disappear in the holaspid pygidia of *Q.*
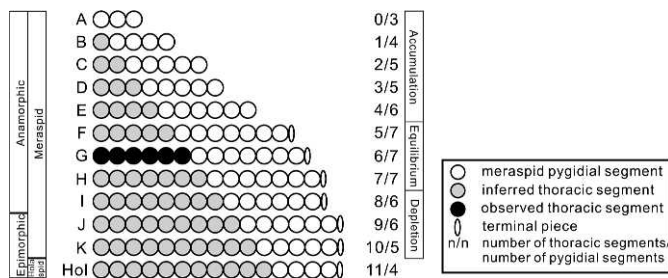

FIGURE 12—The relationship between the developmental stages and the size of the meraspid and earliest holaspid pygidium of *Quadraticephalus elongatus* (Kobayashi, 1935). *A*, scatter plots of pygidial length versus width; *B*, the mean for each stage, and the standard deviation bars extending to horizontal and vertical sides of the mean.

FIGURE 11—Inferred trunk segmentation schedules of *Quadraticephalus elongatus* (Kobayashi, 1935). Cephalon is to the left side in all cases. A through K designate meraspid stages, Hol designates the holaspid period. Open circles represent segments of the pygidium, and grey circles represent inferred thoracic segments, while closed circles represent observed thoracic segments. Ellipse at the end of pygidium represents the terminal piece.
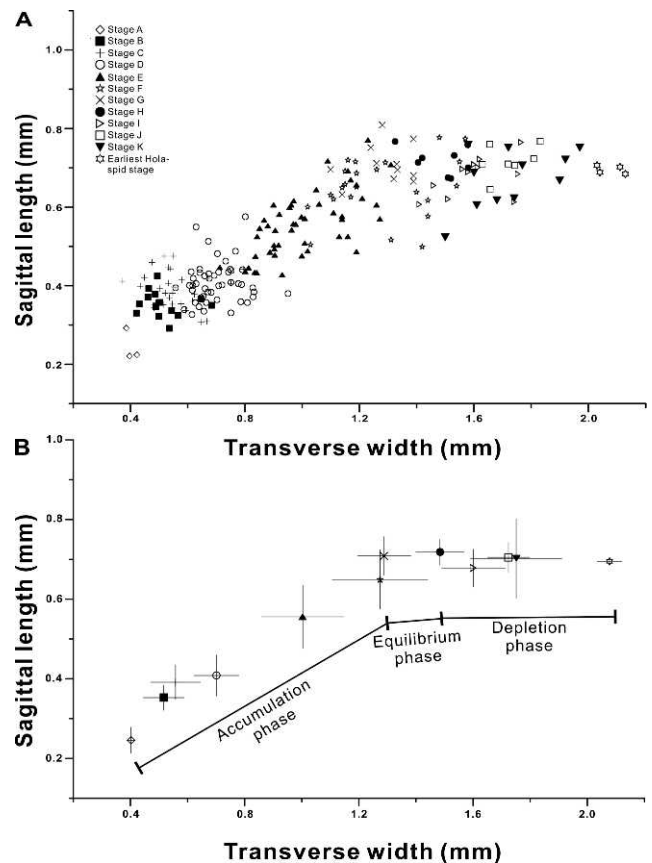
elongatus. In short, a comparison of the ontogeny of the two ptychaspidid species reveals that paedomorphosis played a significant role in the attainment of the mature morphology of *Q. elongatus*.

The meraspid pygidia of *Q. elongatus* are divided into 11 stages according to size and morphology. The number of segments within the meraspid pygidium begins with three and increases to seven (the accumulation phase). Subsequently, it does not change for a while (the equilibrium phase), and eventually decreases to four (the depletion phase). The total number of trunk segments reached its maximum during the beginning of the depletion phase (epimorphic phase) and the holaspid period begins at the end of the depletion phase. Therefore, the developmental mode of *Q. elongatus* is protomeric.

REFERENCES

ADRAIN, J. M. 2011. Class Trilobita Walch, 1771. *In* Z.-Q. Zhang (ed.), Animal biodiversity: An outline of higher-level classification and survey of taxonomic richness. Zootaxa, 3148:104–109.

ADRAIN, J. M., S. E. PETERS, AND S. R. WESTROP. 2009. The Marjuman trilobite *Cedarina* Lochman: thoracic morphology, systematics, and new species from western Utah and eastern Nevada, U.S.A. Zootaxa, 2218:35–58.

CHATTERTON, B. D. E. AND S. E. SPEYER. 1997. Ontogeny, p. 173–247. *In* R. L. Kaesler (ed.), Treatise on Invertebrate Paleontology, Pt. O, Arthropoda 1, Trilobita 1 (Revised). Geological Society of America and University of Kansas Press, Lawrence, Kansas and Boulder, Colorado.

CHOI, D. K. 1998. The Yongwol Group (Cambrian–Ordovician) redefined: a proposal for the stratigraphic nomenclature of the Choson Supergroup. Geoscience Journal, 2:220–234.

CHOI, D. K., S. K. CHOUGH, Y. K. KWON, S.-B. LEE, J. WOO, I. KANG, H. S. LEE, S. M. LEE, J. W. SOHN, Y. J. SHINN, AND D.-J. LEE. 2004. Taebaek Group (Cambrian–Ordovician) in the Seokgaejae section, Taebaeksan Basin: a refined lower Paleozoic stratigraphy in Korea. Geoscience Journal, 8:125–151.

ENDO, R. AND C. E. RESSER. 1937. The Sinian and Cambrian formations and fossils of southern Manchoukuo. Manchurian Science Museum Bulletin, 1:1–474.

FORTEY, R. A. 1990. Ontogeny, hypostome attachment and trilobite classification. Palaeontology, 33:529–576.

FORTEY, R. A. 1997. Late Ordovician trilobites from southern Thailand. Palaeontology, 40:397–449.

FORTEY, R. A. AND B. CHATTERTON. 1988. Classification of the trilobite suborder Asaphina. Palaeontology, 31:165–222.

HUGHES, N. C., A. MINELLI, AND G. FUSCO. 2006. The ontogeny of trilobite segmentation: a comparative approach. Paleobiology, 32:602–627.

KOBAYASHI, T. 1933. Upper Cambrian of the Wuhutsui basin, Liaotung, with special reference to the limit of Chaumitien (or Upper Cambrian) of eastern Asia and its subdivision. Japanese Journal of Geology and Geography, 11:55–155.

KOBAYASHI, T. 1935. The Cambro–Ordovician Formations and Faunas of south Chosen. Palaeontology , Part 3, Cambrian Faunas of south Chosen with a special study on the Cambrian trilobite genera and families. Journal of the Faculty of Science, 4(2):49–344.

KOBAYASHI, T. 1942. Two new trilobite genera, *Hamashania* and *Kirkella*. Journal of the Geological Society of Japan, 59:37–40.

LEE, S. B. AND D. K. CHOI. 2011. Dikelocephalid trilobites from the *Eosaukia* fauna (upper Furongian) of the Taebaek Group, Korea. Journal of Paleontology, 85:279–297.

PARK, T.-Y. AND D. K. CHOI. 2009. Post-embryonic development of the Furongian (late Cambrian) trilobite *Tsinania canens*: implications for life mode and phylogeny. Evolution and Development, 11:441–455.

PARK, T.-Y. AND D. K. CHOI. 2010a. Two middle Cambrian diceratocephalid trilobites, *Cyclolorenzella convexa* and *Diceratocephalus cornutus*, from Korea: development and functional morphology. Lethaia, 43:73–87.

PARK, T.-Y. AND D. K. CHOI. 2010b. Ontogeny and ventral median suture of the ptychaspidid trilobite *Asioptychaspis subglobosa* (Sun, 1924) from the Furongian (upper Cambrian) Hwajeol Formation, Korea. Journal of Paleontology, 84:309–320.

PARK, T.-Y. AND D. K. CHOI. 2011a. Ontogeny of the Furongian (late Cambrian) remopleuridioid trilobite *Haniwa quadrata* Kobayashi, 1933 from Korea: implications for trilobite taxonomy. Geological magazine, 148:288–303.

PARK, T.-Y. AND D. K. CHOI. 2011b. Constraints on using ontogenetic data for trilobite phylogeny. Lethaia, 44:250–254.

SALTER, J. W. 1864. On some new fossils from the Lingula-flags of Wales. Quarterly Journal of the Geological Society, 20(1–2):233–241.

SIMPSON, A. G., N. C. HUGHES, D. C. KOPASKA-MERKEL, AND R. LUDVIGSEN. 2005. Development of the caudal exoskeleton of the pliomerid trilobite *Hintzeia plicamarginis* new species. Evolution and Development, 7:528–541.

SOHN, J. W. AND D. K. CHOI. 2007. Furongian trilobites from the *Asioptychaspis* and *Quadraticephalus* zones of the Hwajeol Formation, Taebaeksan Basin, Korea. Geoscience Journal, 11:297–314.

SUN, Y. C. 1924. Contributions to the Cambrian faunas of North China. Palaeontological Sinica Series B, 1:297–314.

WALCOTT, C. 1905. Cambrian faunas of China. Proceedings of U.S. National Museum, 29:1–106.

WHITTINGTON, H. B. 2003. The upper Cambrian trilobites *Plethopeltis* and *Leiocoryphe*: morphology, paedomorphism, classification. Journal of Paleontology, 77:698–705.

WHITTINGTON, H. B. 2007. Reflections on the classification of the Trilobita. New York State Museum Bulletin, 507:225–230.

WHITTINGTON, H. B. AND S. R. A. KELLY. 1997. Morphological terms applied to Trilobita, p. 313–329. *In* R. L. Kaesler (ed.), Treatise on Invertebrate Paleontology, Pt. O, Trilobita (Revised). Geological Society of America and University of Kansas Press, Lawrence, Kansas.

ZHANG, W. T. AND P. A. JELL. 1987. Cambrian trilobites of North China: Chinese trilobites housed in the Smithsonian Institution. Science Press, Beijing, 459 p.